Chinese Journal of
POLYMER SCIENCE

RESEARCH ARTICLE

https://doi.org/10.1007/s10118-026-3715-5
Chinese J. Polym. Sci. **2026**, *44*, 2880–2890

Multiple-Responsive Chiral Hydrogels from Helical Dendronized Poly(phenylacetylene)s

Lei Wang, Quan-Sheng Li, Lin Yun, Afang Zhang*, and Wen Li*

School of Materials Science and Engineering, Shanghai University, Shanghai 200444, China

Electronic Supplementary Information

Abstract Chiral hydrogels derived from helical polymers are attractive as intelligent chiral materials due to the combination of polymer helicity and hydrogel characteristics. Here, we report the synthesis and characterization of chiral hydrogels from helical thermoresponsive dendronized poly(phenylacetylene)s *via* dynamic covalent acylhydrazone crosslinking, which are responsive to temperature, pH and redox. Two types of helical copolymers, featuring dendritic oligoethylene glycol (OEG) units terminated with either methoxyl or ethoxyl groups, were employed as precursors to afford distinct overall hydrophilicity. These precursors exhibited unprecedented thermoresponsive behavior attributed to the densely grafted dendritic OEGs, with cloud points (T_{cp}s) primarily governed by the terminal groups (methoxyl versus ethoxyl). To impart multi-responsiveness, a disulfide-containing crosslinker was selected for hydrogel formation. Gelation was conducted at three different temperatures—freezing temperature, room temperature (below T_{cp}), and elevated temperature (above T_{cp})—yielding hydrogels with tunable responsiveness to temperature, pH, and redox conditions. The resulting hydrogels displayed stabilized helicity, along with good self-healing properties, excellent compressibility and robust mechanical performance. Preliminary biocompatibility assays indicated low cytotoxicity, underscoring their potential for biomedical applications.

Keywords Helical polymers; Dendronized polymers; Stimuli-responsive polymers; Hydrogels; Chirality

Citation: Wang, L.; Li, Q. S.; Yun, L.; Zhang, A.; Li, W. Multiple-responsive chiral hydrogels from helical dendronized poly(phenylacetylene)s. *Chinese J. Polym. Sci*. **2026**, *44*, 2880–2890.

INTRODUCTION

Multi-responsive hydrogels are highly promising owing to their ability to exhibit tunable properties in response to various external stimuli that induce physical or chemical changes depending on the surrounding environment.[1,2] These stimuli include temperature, pH, redox potential, and light, rendering such hydrogels attractive for application in artificial muscles,[3] actuators[4,5] and intelligent soft electronics.[6–8] In contrast to achiral hydrogels, stimuli-responsive chiral hydrogels possess intrinsic chirality, mimicking the chiral features of biomacromolecules. By integrating hydrogel characteristics with chirality, these materials exhibit environmentally tunable chiral behavior, and have demonstrated significant potential in cell culture and drug delivery.[9] Such chiral hydrogels can be fabricated from peptides or low-molecular-weight chiral molecules *via* supramolecular interactions.[10] However, their major limitation lies in their poor mechanical properties, which has prompted the use of post-crosslinking strategies to enhance their mechanical performance.[11]

Chiral hydrogels derived from helical polymers are particularly interesting.[12,13] These materials combine the inherent characteristics of hydrogels with the unique properties of helical polymers, resulting in enhanced mechanical performance that is suitable for practical biomedical applications.[14] Incorporating stimuli-responsive features into helical polymer hydrogels offers several advantages: (1) tunable responsiveness to environmental changes *via* multiple types of interactions, (2) enhanced chirality originating from helical polymer backbones, (3) improved mechanical robustness, and (4) the potential to fabricate composite hydrogels with tailored compositions. For instance, an interesting class of chiral hydrogels has been developed using high-molar-mass helical polyisocyanides bearing linear oligoethylene glycol (OEG) pendants. These polymers self-assemble into bundled structures upon thermal dehydration, yielding chiral hydrogels with tunable mechanical properties *via* post-crosslinking strategies.[15–18] Nevertheless, stimuli-responsive chiral hydrogels based on helical polymers are predominantly limited to thermoresponsive behavior, which restricts their potential utility in applications, such as chiral actuators and biomedicine.[15,19]

Recently, we reported a novel class of chiral hydrogels derived from thermoresponsive helical-dendronized poly-

* Corresponding authors, E-mail: azhang@shu.edu.cn (A.Z.)
E-mail: wli@shu.edu.cn (W.L.)
Special Topic: Chirality in Polymers
Received March 1, 2026; Accepted April 14, 2026; Published online June 22, 2026

(phenylacetylene)s (PPAs), which exhibited intriguing sponge-like compression behavior.[20] These hydrogels retained their thermoresponsive properties compared to the dendronized PPA precursors.[21–24] In contrast to the free dendronized PPAs, which displayed tunable helicity depending on the solvation conditions,[25,26] the hydrogels exhibited stabilized helicity owing to the increased conformational constraints introduced by interchain crosslinking. Their reversible deformation behavior can be suppressed and fixed *via* solvent exchange with water-immiscible solvents such as dichloromethane (DCM). Owing to their reversible compressibility and excellent fatigue resistance, these hydrogels were employed as soft actuators to modulate electrical conductivity through stress-induced deformation.[27] By integrating thermoresponsive helical polymers with dynamic covalent acylhydrazone linkages and disulfide bonds derived from the crosslinker, we here report on fabrication of a class of multi-responsive chiral hydrogels. These hydrogels inherit the chirality of the helical PPA precursors and exhibit unprecedented thermoresponsive behavior originating from dendritic oligoethylene glycol (OEG) moieties.[28–34] Furthermore, they undergo reversible sol–gel transitions in response to redox stimuli, enabled by disulfide bonds, as well as pH changes owing to the presence of acylhydrazone linkages.

EXPERIMENTAL

Materials

Poly(Me$_m$-*co*-EB$_n$) and **Poly(Et$_m$-*co*-EB$_n$)** copolymers were synthesized according to our previous reports.[20,21] Triethylamine (TEA), triethylene glycol monomethyl ether, alkynyl benzaldehyde (**EB**), and dimethyl 3,3'-dithiodipropionate were purchased from TCI (Japan). Dichloromethane (DCM) was distilled from CaH_2 and dried. Tetrahydrofuran (THF) was distilled from $LiAlH_4$ and sodium for drying. All reactions were performed under a nitrogen atmosphere. Other reagents and solvents were of reagent grade and used as received. Macherey-Nagel precoated TLC plates (silica gel 60 G/UV254, 0.25 mm) were used for thin-layer chromatography (TLC) analysis. Silica gel 60 M (Macherey-Nagel, 0.040–0.063 mm, 200–300 mesh) was used as the stationary phase for the column chromatography.

Instrument and Measurements

^{1}H-NMR spectra were recorded using a Bruker AV 500 (^{1}H: 500 MHz). Size exclusion chromatography (SEC) measurements were performed on a Waters GPC e2695 instrument with a three-column set (Styragel HR3 + HR4 + HR5) equipped with a refractive index detector (Waters 2414) at 45 °C. DMF (containing 1 g·L^{-1} of LiBr) was used as eluent. Circular dichroism (CD) measurements were performed on a JASCO J-815 spectropolarimeter with a thermo-controlled 1 mm quartz cell (three accumulations, "continue scanning" mode, scanning speed: 200 nm·min^{-1}; data pitch: 0.2 nm; response: 1 s; bandwidth: 2.0 nm). UV/vis spectroscopy and turbidity measurements were performed using a JASCO UV/Vis spectrophotometer (V-750). The aqueous polymer solutions were placed in a spectrophotometer (path length 1 cm) and heated or cooled at a rate of 0.2 °C·min^{-1}. The absorption of the solutions was recorded at λ = 700 nm for 5 s. The cloud point (T_{cp}) was determined to be the point at which the transmittance at 700 nm reached 50% of its initial value. The pH was measured using a Mettler-Toledo Seven Compact 220 pH meter and an InLab Flex-Micro semi-micro electrode (after 4 points calibration at pH 10.00, 7.00, 4.01, and 2.00). Rheological experiments were carried out using a rheometer (MCR 302, Anton Paar Instruments, Austria) with a parallel plate (diameter, 15 mm) configuration. The strain was fixed at 0.5%, and frequency scanning tests were conducted within a frequency range of 0.1–100 rad·s^{-1}. The sample thickness was 1 mm, and a flat rotor with a diameter of 15 mm was used. The test temperature was maintained at 25 °C. The lyophilized hydrogel samples were examined and digital micrographs were acquired using a scanning electron microscope (HITACHI SU-1510, Japan). The hydrogel samples were platinum-coated and mounted with carbon adhesive tape on iron specimens.

General Procedure for Preparation of the Dendronized Copolymer Hydrogels

An aqueous solution of the copolymer (20 mg) was dissolved in PBS buffer (pH=5) and incubated for 24 h. Subsequently, the crosslinker 3,3'-dithiobis(propionohydrazide) (**CS-*S***, with a molar ratio of amino groups to aldehyde groups in the copolymer of 1.5:1) was added, followed by stirring for 30 s. The mixture was allowed to gel at three different temperatures for 12 h, affording the corresponding hydrogels.

Multi-Stimuli Responsiveness of the Hydrogels

pH-responsive sol-gel transitions of the hydrogels were investigated by alternately adding HCl (30 μL, 17.5 mol·L^{-1}) and TEA (60 μL, 7.2 mol·L^{-1}); this process was repeated for three to four cycles. Subsequently, the redox-responsive behavior of the hydrogels was explored as follows: addition of DTT (6 mg) and H_2O_2 (20 μL) induced a reversible sol-gel transition, a process that was repeated for three to four cycles.

RESULTS AND DISCUSSION

Synthesis and Characterization of Copolymer Precursors

The copolymer precursors were designed to have the same PPA backbone but with different pendants. As shown in Scheme 1, dendritic OEGs bearing either methoxyl or ethoxyl terminals contribute to copolymer water solubility and different thermoresponsiveness, while the aldehyde moiety is used to react with the acylhydrazine crosslinker to form quantitative acylhydrazones for crosslinking.[35] As demonstrated previously, hydrogels formed through dynamic covalent linkages avoid heterogeneous structures compared to those formed through photo-crosslinking.[36–38] The compositions of these copolymers were designed for the ratio of the dendritic pendants and aldehyde moieties in the range of 50:1 to 10:1, ensuring the crosslinking density of the formed hydrogels and appropriate amounts of dendritic and chiral pendants to guarantee the thermoresponsive properties and helicity of the resulting copolymers. These copolymers were prepared with R_h catalyst at ambient temperature with good yields, and their molar masses were in the range of half million (Table 1). Based on the proton signals in the ^{1}H-NMR spectra (Figs. S1–S5 in the electronic supplementary information, ESI), the compositions of the copolymers were calculated and found to be similar to those of the designed copolymers.

https://doi.org/10.1007/s10118-026-3715-5

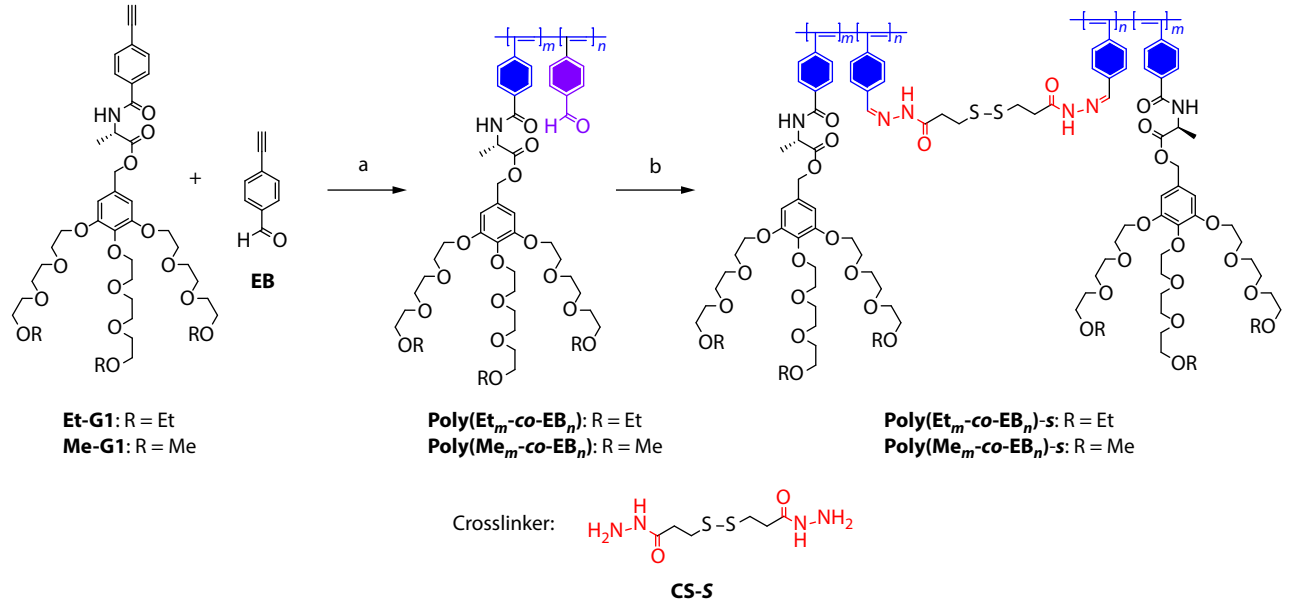

Scheme 1 Synthetic routes for the dendronized phenylacetylene copolymers and their crosslinking with hydroxylamine to form the corresponding chiral hydrogels. Reagents and conditions: (a) **Me-PA** or **Et-PA**, **EB**, $[Rh(nbd)Cl]_2$, TEA, THF, r.t., 12 h (80%–85%); (b) Copolymer (10 wt%), the crosslinker **CS-*S*** (NH_2/CHO = 1.5), water, overnight (90 wt%). Abbreviations: **CS-*S*** = 3,3'-dithiobis(propiono-hydrazide); **EB** = 4-ethynylbenzaldehyde; TEA = triethylamine.

Table 1 Polymerization conditions and results for the copolymers. [a]

Copolymer sample	Composition ratio [Dendritic PA]/[**EB**]		Yield (%)	SEC results [c]		T_{cp} [d] (°C)
	Monomer	Copolymer [b]		M_n×10^{-4} (Da)	$Đ$	
Poly(Me$_8$-*co*-EB$_1$)	9:1	8:1	82	51.9	2.15	54.6
Poly(Me$_{25}$-*co*-EB$_1$)	19:1	25:1	79	53.1	2.04	55.4
Poly(Me$_{51}$-*co*-EB$_1$)	49:1	51:1	84	44.3	1.74	55.9
Poly(Et$_{11}$-*co*-EB$_1$)	9:1	11:1	78	47.2	1.96	27.6
Poly(Et$_{25}$-*co*-EB$_1$)	19:1	25:1	85	51.2	1.86	29.7

[a] Polymerization was performed using $[Rh(nbd)Cl]_2$ (nbd: norbornadiene) as the catalyst in THF at 25 °C in the presence of TEA with [monomer]/[TEA]/$[Rh(nbd)Cl]_2$ = 300/300/1; [b] Compositions were obtained from proton integrations in ^{1}H-NMR spectra; [c] Determined by SEC with DMF as the eluent containing 0.1 wt% LiBr. M_n and $Đ$ represent number-average molecular weight and polydispersity, respectively; [d] Apparent T_{cp}s of the copolymers were determined to be the temperature at 50% of the initial transmittance at λ = 700 nm.

Because of the densely grafted dendritic OEGs, these copolymers inherited unprecedented thermoresponsive behaviors from the OEG dendrons, and their thermoresponsive properties were followed by turbidimetry. As shown in Fig. 1(a), these copolymers exhibited sharp phase transitions with a small hysteresis between heating and cooling. Their cloud points (T_{cp}s) are mainly dependent on the terminal units of the dendrons (either methoxyl or ethoxyl), which are less relevant to their compositions. For those carrying methoxyl-terminated OEG dendrons, T_{cp}s was approximately 55 °C. For these ethoxyl-terminated OEG dendrons, T_{cp}s was much lower and was around 30 °C. Compared to their counterparts with polymethacrylate backbones, which were reported previously,[28,29] these copolymers showed slightly lower T_{cp}s, indicating that the hydrophobic PPA backbones from these copolymers contribute to a certain degree of hydrophobicity to alter their thermoresponsive behaviors.

The chiroptical properties of these copolymers were examined by CD spectroscopy, and their CD spectra at various temperatures across the thermal phase transitions are shown in Figs. 1(b) and 1(c). Copolymers with either hydrophilic methoxyl or more hydrophobic ethoxyl terminals exhibited a characteristic Cotton effect at approximately 370 nm, corresponding to the polyene backbone. This indicates backbone helicities. However, these copolymers exhibited different helicity inversions across their thermal phase transitions (Fig. 1d). For copolymers bearing hydrophilic methoxy terminals, the negative Cotton effects at room temperature were inverted into positive ones at elevated temperatures. However, for copolymers bearing more hydrophobic ethoxyl terminals, the positive Cotton effects at room temperature inverted into negative ones at elevated temperatures. The helicity transformation of these copolymers during their thermal phase transitions indicates that they adopt dynamic helical conformations according to the thermal dehydration-mediated solvation difference, similar to the conventional PPAs that adopt varied helicities according to solvation.[39–46]

Fabrication and Characterization of the Chiral Hydrogels

A crosslinker (**CS-*S***) with a disulfide linkage was used to fabricate hydrogels from these helical dendronized copolymers

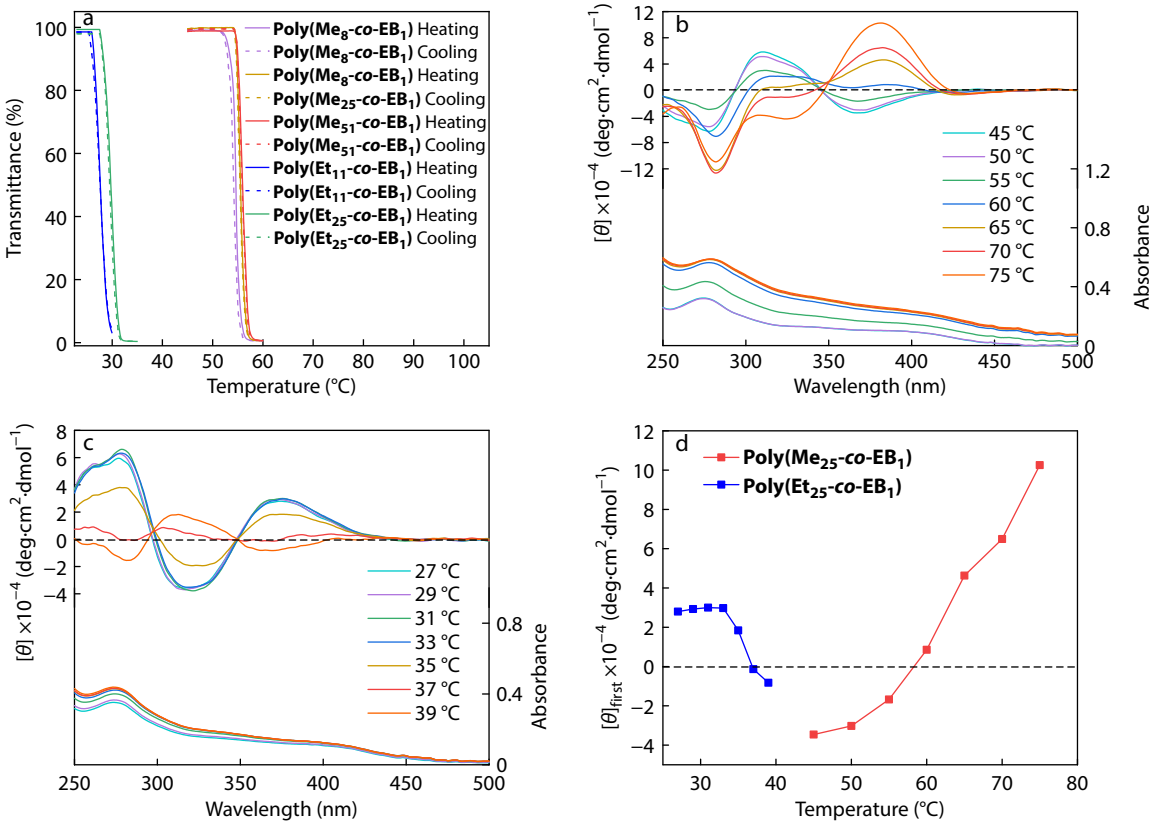

Fig. 1 Turbidity curves of **Poly(Me$_m$-*co*-EB$_n$)** and **Poly(Et$_m$-*co*-EB$_n$)** (a). c = 0.5 mg·mL^{-1}. Heating and cooling rate = 0.5 °C·min^{-1}. CD-UV/Vis spectra from the aqueous solutions of copolymers **Poly(Me$_{25}$-*co*-EB$_1$)** (b) and **Poly(Et$_{25}$-*co*-EB$_1$)** (c) at different temperatures. c = 0.25 mg·mL^{-1}. Heating and cooling rate = 0.5 °C·min^{-1}. Dot line was added for eye-guiding. Plots of the first cotton effect ($[\theta]_{first}$) against temperature from aqueous solutions of polymers **Poly(Me$_{25}$-*co*-EB$_1$)** and **Poly(Et$_{25}$-*co*-EB$_1$)** (d).

(Scheme 1) to ensure multiple responsiveness to the formed chiral hydrogels. This crosslinker was synthesized from dimethyl 3,3'-dithiodipropionate through hydrazination according to a previously reported method.[47] In addition to the thermoresponsive behavior inherited from dendritic OEGs, these hydrogels also exhibit redox- and pH-responsive properties originating from disulfide and acylhydrazone linkages. Helical copolymers can be readily transformed into chiral hydrogels through acylhydrazone formation *via* the reaction of acylhydrazines from the crosslinker **CS-*S*** with aldehydes from the copolymers.[20] Three different temperatures were used to fabricate the hydrogels: freezing temperature, room temperature (below the T_{cp}), and elevated temperature (above the T_{cp}), aiming at hydrogels with varied morphologies and different mechanical properties. For the hydrogels formed at freezing temperatures, crosslinking was performed among the concentrated copolymer chains templated by ice, which led to the formation of highly porous hydrogels. For hydrogels prepared at room temperature, crosslinking was performed among the distributed copolymer chains in water, which may lead to the formation of homogeneous hydrogels. For the hydrogels formed at elevated temperatures, crosslinking occurred among the thermally aggregated copolymer chains, which should lead to the formation of hydrogels with varied morphologies.

The morphologies of the hydrogels were characterized using laser scanning confocal microscopy (LSCM).[48–50] Because of the high rigidity of the densely pendanted OEG dendrons, these dendronized PPAs showed stronger fluorescence than conventional PPAs; therefore, the corresponding hydrogels can be directly visualized in LSCM without additional fluorescent agents. As shown in Fig. 2, the hydrogel morphology was mainly dependent on the fabrication temperature. Hydrogels formed at freezing temperatures from both **Poly(Me$_8$-*co*-EB$_1$)** and **Poly(Et$_{11}$-*co*-EB$_1$)** showed similar membraned microporous morphologies, whereas hydrogels formed at room temperature showed more homogeneous structures. The hydrogels formed at elevated temperatures adopted heterogeneous morphologies compared with those formed at room temperature. Their morphologies were further examined using scanning electron microscopy (SEM). As shown in Fig. 3, similar results were obtained, and the hydrogels formed at freezing temperatures exhibited extensive microporous morphologies. Although both methoxyl- and ethoxyl-terminated copolymers possessed slightly different hydrophilicities, the corresponding hydrogels prepared at temperatures well below their cloud points exhibited similar morphologies. This suggests that crosslinking among copolymers at either room temperature or freezing temperature does es not contribute much to the formation of hydrogels, except that crosslinking at freezing temperature was processed in concentrated copolymers compared to that at room temperature. This is different from the gelation above the cloud points, where copolymers were aggregated first through thermal dehydration and collapse, followed by *in situ*

https://doi.org/10.1007/s10118-026-3715-5

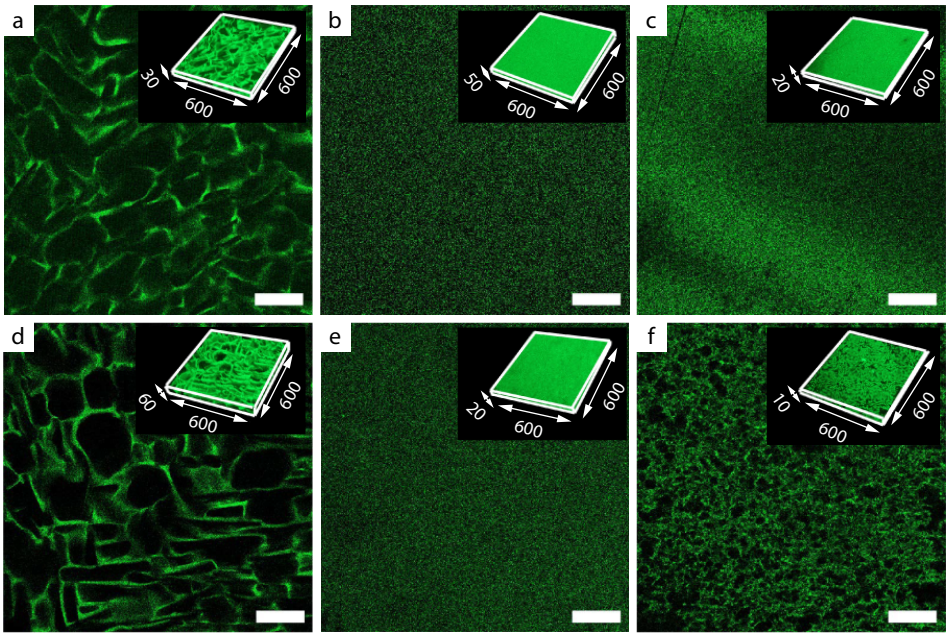

Fig. 2 LSCM images of the hydrogels **Poly(Me$_8$-*co*-EB$_1$)-*s*** prepared at −20 °C (a), 25 °C (b) and 56 °C (c), respectively, as well as these **Poly(Et$_{11}$-*co*-EB$_1$)-*s*** prepared at −20 °C (d), 25 °C (e) and 30 °C (f), respectively. Insets are the three-dimensional images accumulated with ZEN blue software from the corresponding one-dimensional images. Wavelength of irradiation light was 488 nm. Scale bars are 100 μm.

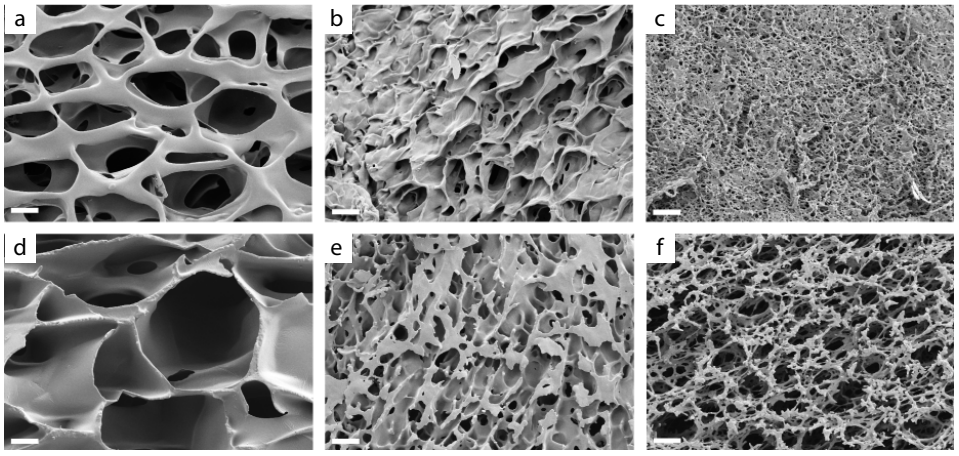

Fig. 3 SEM images of the hydrogels **Poly(Me$_8$-*co*-EB$_1$)-*h*** prepared at −20 °C (a), 25 °C (b), and 56 °C (c), and the hydrogels **Poly(Et$_{11}$-*co*-EB$_1$)-*h*** prepared at −20 °C (d), 25 °C (e), and 30 °C (f), respectively. All hydrogels (10 wt%) were freeze-dried prior to SEM characterization. Scale bars are 20 μm.

crosslinking among the aggregates to form hydrogels. Different radial amphiphilicities between methoxyl- and ethoxyl-terminated copolymers[22,23] led to varied aggregations of different morphologies in the hydrogels. The porosities of the hydrogels formed at different temperatures were analyzed according to a literature method [51] and the results are summarized in Table S1 (in ESI). The hydrogels formed at freezing temperatures possessed highest porosity (about 81%), and those formed at elevated temperatures showed porosity around 68%. However, the hydrogels formed at room temperature possessed much lower porosities (about 50%). This indicates that the porosities of the hydrogels can be modulated by simply controlling the formation temperature. For the hydrogels formed at freezing temperatures, the copolymer precursors were concentrated with ice as the template for crosslinking network formation, leading to the formation of microporous membranes with high porosity. For the hydrogels formed at elevated temperatures, the copolymer precursors first dehydrated and collapsed to form mesoglobules[29] and crosslinking was performed among the aggregates. In contrast, for hydrogels formed at room temperature, crosslinking was achieved from individually distributed polymer chains, resulting in a more homogeneous morphology with the smallest porosities.

The chiroptical properties of hydrogels formed at different temperatures were analyzed using CD spectroscopy. As shown in Fig. 4, the helicities of the hydrogels prepared at either freezing or elevated temperatures remained the same during the thermal phase transitions, which contrasts with the copolymer precursors that underwent helicity inversion

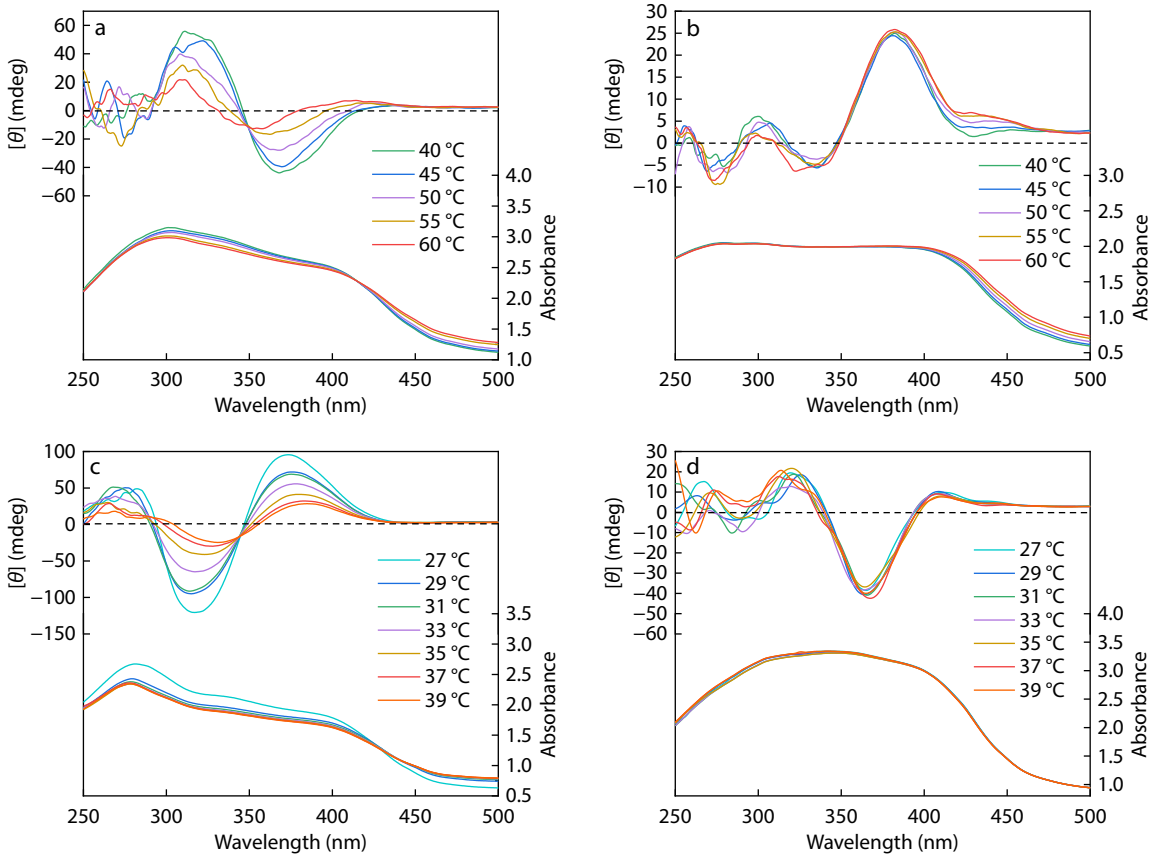

Fig. 4 Temperature-dependent CD-UV/Vis spectra of hydrogel **Poly(Me$_{25}$-*co*-EB$_1$)-*s*** prepared at −20 °C (a) and hydrogel **Poly(Me$_{25}$-co-EB$_1$)-*s*** prepared at 56 °C (b). Temperature-dependent CD-UV/Vis spectra of hydrogel **Poly(Et$_{25}$-*co*-EB$_1$)-*s*** prepared at −20 °C (c) and hydrogel **Poly(Et$_{25}$-*co*-EB$_1$)-*s*** prepared at 30 °C (d). The solid content of the hydrogels was 5 wt%. pH = 5.

across their cloud points. This indicates that crosslinking provides sufficient barriers to prevent the inversion of helicities, in contrast to the dynamic helictites of the copolymer precursors, as shown in Fig. 1. However, the helicity stabilization of hydrogels is related to the fabrication temperature. For the hydrogels formed at freezing temperature from both ethoxyl- and methoxyl-terminated copolymers, the intensities of the first Cotton effects diminished with increasing temperature (Figs. 4a and 4c). For the hydrogels formed at elevated temperatures, the intensities of the first Cotton effects remained the same for both ethoxyl- and methoxyl-terminated copolymers when the temperature increased across their thermal phase transitions (Figs. 4b and 4d). This indicates that hydrogels formed at elevated temperatures can provide an enhanced conformational barrier for isomerization of the polyene backbone. Hydrogels prepared at elevated temperatures were formed through crosslinking of thermally induced copolymer aggregates. Dehydrated and collapsed copolymer chains within the thermal aggregates were densely packed, which is not only helpful for crosslinking through close chain contact but also supports entanglement to impose stronger spatial constraints on the polymer chains. Both should have contributed to stabilizing the helicities of the resulting hydrogels.

Properties of the Chiral Hydrogels

The viscoelastic properties of these chiral hydrogels were investigated using dynamic rheology measurements on a rotational rheometer, and it was found that their mechanical properties were dominated by the gelation temperatures. As shown in Fig. 5, with **Poly(Me$_m$-*co*-EB$_n$)-*s*** as an example, the hydrogels showed different mechanical properties according to their gelation temperature and composition. For the samples prepared at room temperature, as shown in Figs. 5(a) and 5(b), G' was approximately 240 Pa. In contrast, the hydrogels prepared at freezing temperatures showed a significant increase in G' in the range of 2650 Pa. For the hydrogels prepared at elevated temperatures above T_{cp}, their G's were further increased to 3300 Pa. Comparing the hydrogels from copolymers with different compositions, as shown in Fig. 5(c), G' increased significantly from 477 Pa for **Poly(Me$_{51}$-*co*-EB$_1$)-*s*** to 1996 Pa for **Poly(Me$_{25}$-*co*-EB$_1$)-*s*** and 2650 Pa for **Poly(Me$_8$-*co*-EB$_1$)-*s***, indicating that the high crosslinking density in **Poly(Me$_8$-*co*-EB$_1$)-*s*** is helpful to ensure that the hydrogel has better mechanical properties. Hydrogels from ethoxyl-terminated copolymers showed similar temperature-dependent tendencies for their mechanical properties to those formed from methoxyl-terminated copolymers. However, the mechanical properties of the hydrogels from **Poly(Et$_{11}$-*co*-EB$_1$)** were much weaker than those of their methoxyl-terminated counterparts, as shown in Fig. 5(d).

Similar to our previous reports,[20,27] these hydrogels also exhibited intriguing compression resistance. As shown in Fig. 5(e), both **Poly(Me$_8$-*co*-EB$_1$)-*s*** and **Poly(Et$_{11}$-*co*-EB$_1$)-*s*** pre-

https://doi.org/10.1007/s10118-026-3715-5

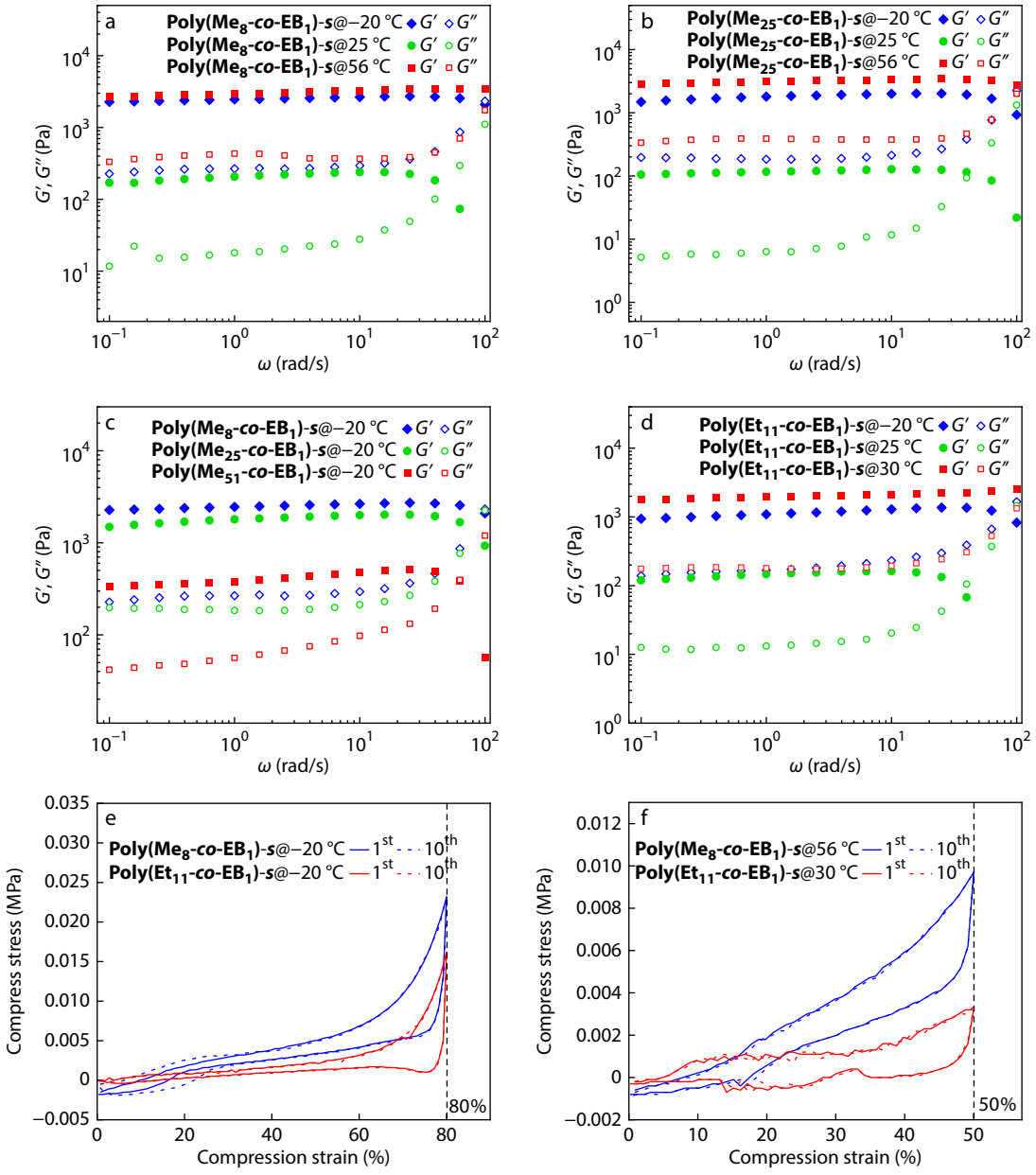

Fig. 5 Rheological curves of hydrogels **Poly(Me$_8$-*co*-EB$_1$)-*s*** (a) and **Poly(Me$_{25}$-*co*-EB$_1$)-*s*** (b) and **Poly(Et$_{11}$-*co*-EB$_1$)-*s*** (d) prepared at different temperatures; Rheological curves of hydrogels **Poly(Me$_m$-*co*-EB$_n$)-*s*** (c) prepared at –20 °C; The compression stress-strain for the hydrogels **Poly(Me$_8$-*co*-EB$_1$)-*s*** and **Poly(Et$_{11}$-*co*-EB$_1$)-*s*** prepared at –20 °C with 80% strain for 10 cycles (e); The compression stress-strain for the hydrogels **Poly(Me$_8$-*co*-EB$_1$)-*s*** and **Poly(Et$_{11}$-*co*-EB$_1$)-*s*** prepared at phase transition temperature with 50% strain for 10 cycles (f). The solid content of hydrogels was 10 wt%. pH = 5. [NH_2]/[CHO] = 1.5.

pared at freezing temperature showed excellent compression reversibility. After compressions to 80% for 10 times, the plots of compression stresses against compression strain for these hydrogels superimposed, demonstrating excellent fatigue resistance to compression and efficient rehydration. However, this compression reversibility was much worse for hydrogels prepared at elevated temperatures. As shown in Fig. 5(f), both hydrogels **Poly(Me$_8$-*co*-EB$_1$)-*s*** and **Poly(Et$_{11}$-*co*-EB$_1$)-*s*** prepared at elevated temperatures could only resist to 50% compression strain. This suggests that the membraned porous morphology of the cryogels facilitates dehydration under external stress and efficient rehydration after stress removal, resulting in excellent sponge-like behaviors for the hydrogels to show excellent compression reversibility.

The multi-responsive properties of the chiral hydrogels were also investigated. These hydrogels inherited their thermoresponsive behavior from their copolymer precursors. As shown in Fig. S6 (in ESI), the hydrogels from both **Poly(Me$_8$-*co*-EB$_1$)** and **Poly(Et$_{11}$-*co*-EB$_1$)** formed at freezing or elevated temperatures exhibited typical thermal shrinkage and deswelling upon heating. Owing to the presence of acylhydrazone from the copolymers and disulfide linkages from the crosslinker, these hydrogels also exhibited responsiveness to acid/base and redox reactions. For convenience, hydrogels

https://doi.org/10.1007/s10118-026-3715-5

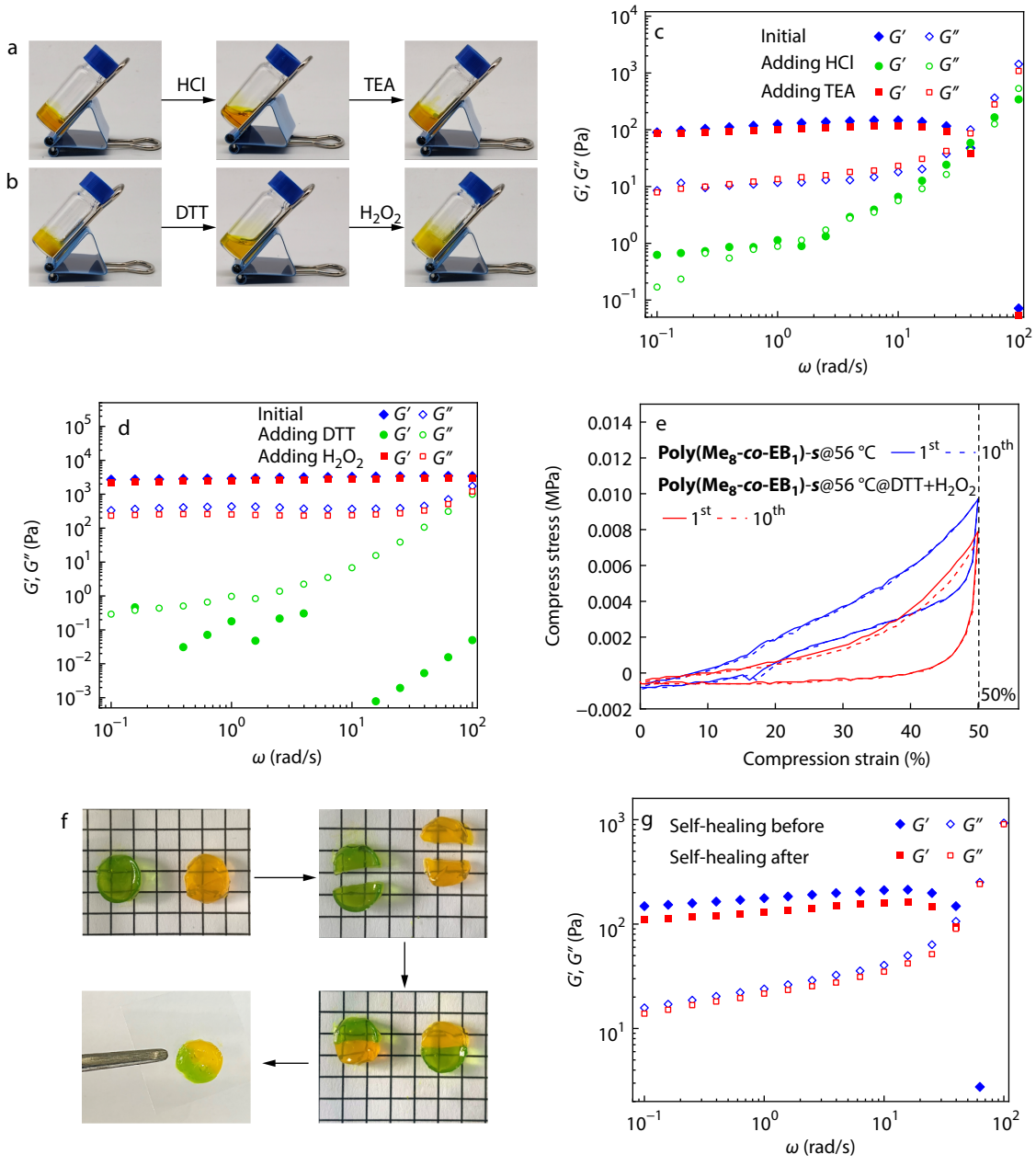

Fig. 6 Sol-gel transitions of hydrogel **Poly(Me$_8$-*co*-EB$_1$)-*s*** prepared at 25 °C in response to pH (a); Sol-gel transitions of hydrogel **Poly(Me$_8$-*co*-EB$_1$)-*s*** prepared at 56 °C in response to redox (b); Rheological curves of hydrogel **Poly(Me$_8$-*co*-EB$_1$)-*s*** prepared at 25 °C before and after pH response (c); Rheological curves of hydrogel **Poly(Me$_8$-*co*-EB$_1$)-*s*** prepared at 56 °C before and after redox reactions (d); Cyclic compression curves of the hydrogel **Poly(Me$_8$-*co*-EB$_1$)-*s*** prepared at 56 °C before and after redox reactions (e); Self-healing photographs of the hydrogel **Poly(Et$_{11}$-*co*-EB$_1$)-*s*** prepared at 25 °C (f) and the related rheological curves (g). One piece of the hydrogels was colored with methylene blue for clarity. Solid content = 10 wt%. pH = 5. [NH_2]/[CHO] = 1.5.

prepared at room temperature are used to illustrate this principle. As shown in Fig. 6(a) for **Poly(Me$_8$-*co*-EB$_1$)-*s***, its gel-sol transition can be modulated by the addition of an acid due to the sensitivity of acylhydrazone linkages to solution pH, which was transformed into a gel again through the addition of a base. Similarly, the sol-gel transitions of **Poly(Me$_8$-*co*-EB$_1$)-*s*** can also be modulated by redox reactions. Redox responsiveness can occur for hydrogels prepared at three distinct temperatures, but the hydrogels prepared above the phase transition temperature exhibited a faster reaction rate; therefore, the redox behavior was focused on hydrogels prepared at 56 °C (above the cloud point). As shown in Fig. 6(b), the gel was transformed into sol through the addition of DTT due to the breakage of the disulfide bonds, which returned to the gel through the addition of hydroperoxide due to the reformation of disulfide bonds. To demonstrate the reversibility of the sol-gel transitions mediated by pH and redox, the viscoelastic properties of the recovered hydrogels were examined using rheology measurements. As shown in Fig. 6(c), the reformed hydrogel possessed a G' similar to that of the hydro-

https://doi.org/10.1007/s10118-026-3715-5

gel before acid-base treatment. The recovery of hydrogels through redox reactions is also efficient. As shown in Fig. 6(d), the reformed hydrogel showed the same *G'* value as the hydrogel before redox treatment. After the redox treatment, the hydrogel exhibited compression reversibility similar to that of the untreated hydrogels (Fig. 6e), illustrating the excellent pH-responsive behavior of these chiral hydrogels toward pH or redox. In addition, the self-healing properties of these chiral hydrogels were preliminarily tested. The self-healing properties of the hydrogels prepared at room temperature were tested owing to their softness. Hydrogels prepared at either freezing temperatures or above the cloud point were quite tough because of the excellent mechanical properties shown in Fig. 5, which is not convenient for self-healing tests. As shown in Fig. 6(f), after cutting into two pieces and pressing the fractured surfaces together, two different pieces of hydrogel merged to form a single piece, which exhibited similar G' as the original hydrogel (Fig. 6g).

To demonstrate the biocompatibility and potential bio-applications of these multiple-responsive chiral hydrogels, their cytotoxicity was examined using the breast cancer cell line MCF-7, and both hydrogels **Poly(Me$_8$-*co*-EB$_1$)-*s*** and **Poly(Et$_{11}$-*co*-EB$_1$)-*s*** prepared at −20 °C were used as examples. As shown in Fig. S7 (in ESI), green fluorescence indicates live cells, and red or bright yellow fluorescence indicates dead or apoptotic states. Cells were encapsulated in the porous holes within both types of the hydrogels and showed high viability after cell culture for one to three days, and maintained viability approaching 100% in both hydrogels within one week of continuous culture. These preliminary results indicate that these helical dendronized hydrogels are good candidates for use in 3D environments for bio-applications. Further exploration of these hydrogels for bioapplications is currently underway by our group.

CONCLUSIONS

Chiral hydrogels were fabricated through covalent dynamic acylhydrazone crosslinking of thermoresponsive helical dendronized poly(phenylacetylene)s (PPAs) at varying temperatures, yielding materials with stabilized chirality, distinct morphologies, and tunable mechanical properties. These hydrogels exhibited redox responsiveness due to the disulfide linkages in the crosslinker, enabling reversible sol–gel transitions. In addition, the dynamic nature of acylhydrazone bonds facilitates pH-induced reversible sol–gel transitions. Crosslinking introduces increased conformational barriers, resulting in stabilized helicity with no helicity inversion observed during thermal phase transitions. Hydrogels prepared at freezing temperatures exhibit a membrane-like porous morphology, which promotes efficient dehydration under external stress and rehydration upon stress release, imparting sponge-like compressibility. This behavior may render these hydrogels attractive for application in mechanical energy storage and energy transfer. Preliminary experiments confirmed that the chiral hydrogels were biocompatible and exhibited low cytotoxicity. Based on their multi-responsive characteristics, we anticipate that these chiral hydrogels will find promising applications in bioactuators and biomedicine.

Conflict of Interests

The authors declare no interest conflict.

Electronic Supplementary Information

Electronic supplementary information (ESI) is available free of charge in the online version of this article at http://doi.org/10.1007/s10118-026-3715-5.

Data Availability Statement

The data supporting the findings of this study are available from the corresponding author upon reasonable request.

ACKNOWLEDGMENTS

This work was financially supported by the National Natural Science Foundation of China (Nos. 22371179 and 22271183) and the Shanghai Oriental Talent Program-Top Talent Project (No. BJJY2024035). We thank Ruitong Jia and Yuexin Cao for their generous contributions to some experiments.

REFERENCES

1 Lee, K. Y.; Mooney, D. J. Hydrogels for tissue engineering. *Chem. Rev.* **2001**, *101*, 1869–1879.
2 Koetting, M. C.; Peters, J. T.; Steichen, S. D.; Peppas, N. A. Stimulus-responsive hydrogels: theory, modern advances, and applications. *Mater. Sci. Eng. R* **2015**, *93*, 1–49.
3 Zhang, X.; Aziz, S.; Salahuddin, B.; Zhu, Z. Thermoresponsive hydrogel artificial muscles. *Matter* **2023**, *6*, 2735–2775.
4 Le, X.; Lu, W.; Zhang, J.; Chen, T. Recent progress in biomimetic anisotropic hydrogel actuators. *Adv. Sci.* **2019**, *6*, 1801584.
5 Na, H.; Kang, Y.-W.; Park, C. S.; Jung, S.; Kim, H. Y.; Sun, J. Y. Hydrogel-based strong and fast actuators by electroosmotic turgor pressure. *Science* **2022**, *376*, 301–307.
6 Liu, X.; Liu, J.; Lin, S.; Zhao, X. Hydrogel machines. *Mater. Today* **2020**, *36*, 102–124.
7 López-Díaz, A.; Vázquez, A. S.; Vázquez, E. Hydrogels in soft robotics: past, present, and future. *ACS Nano* **2024**, *18*, 20817–20826.
8 Hui, Y.; Yao, Y.; Qian, Q.; Luo, J.; Chen, H.; Qiao, Z.; Yu, Y.; Tao, L.; Zhou, N. Three-dimensional printing of soft hydrogel electronics. *Nat. Electron.* **2022**, *5*, 893–903.
9 Dou, X.-Q.; Feng, C.-L. Amino acids and peptide-based supramolecular hydrogels for three-dimensional cell culture. *Adv. Mater.* **2017**, *29*, 1604062.
10 Dou, X.; Mehwish, N.; Zhao, C.; Liu, J.; Xing, C.; Feng, C. Supramolecular hydrogels with tunable chirality for promising biomedical applications. *Acc. Chem. Res.* **2020**, *53*, 852–862.
11 Mei, W.; Li, W.; Zhang, A. Supramolecular assembly of dendronized diacetylenes into thermoresponsive chiral fibers and their covalent fixation through topochemical polymerization. *J. Colloid Interface Sci.* **2024**, *669*, 314–326.
12 Ishikawa, M.; Taura, D.; Maeda, K.; Yashima, E. An optically active hydrogel composed of cross-linked poly(4-carboxyphenyl isocyanide) with a macromolecular helicity memory. *Chem. Lett.* **2004**, *33*, 550–551.
13 Du, X.; Liu, J.; Deng, J.; Yang, W. Synthesis and chiral recognition of optically active hydrogels containing helical polymer chains. *Polym. Chem.* **2010**, *1*, 1030–1038.

Graphical Abstract

Multiple-Responsive Chiral Hydrogels from Helical Dendronized Poly(phenylacetylene)s

Lei Wang, Quan-Sheng Li, Lin Yun, Afang Zhang, and Wen Li

Shanghai University

Chiral hydrogels were fabricated from helical dendronized poly(phenylacetylene)s through acylhydrazone linkage with a disulfide crosslinker. They exhibited responsiveness to temperature, pH, and redox, and possessed characteristic stabilized helicity, reversible compression, and low cytotoxicity.

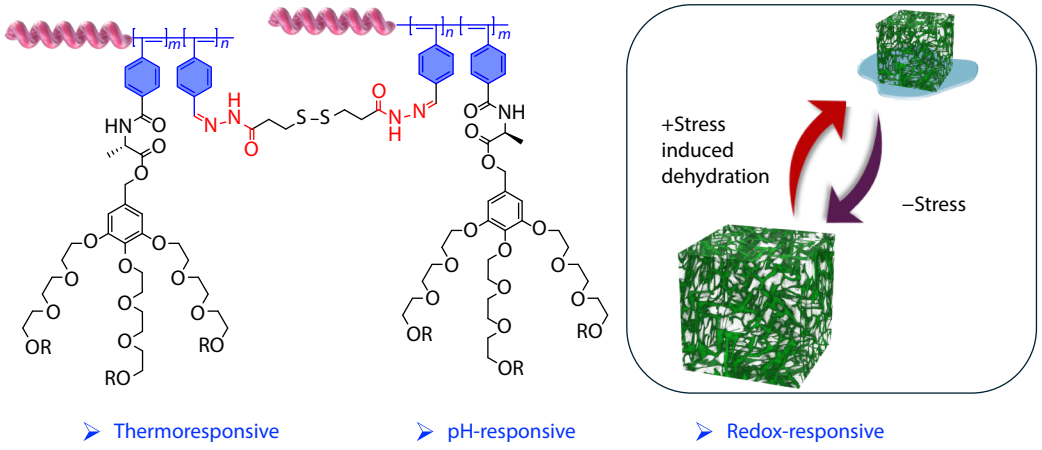

Chinese J. Polym. Sci. 2026, 44, 2880–2890 *https://doi.org/10.1007/s10118-026-3715-5*

14 Yao, F.; Zhang, D.; Zhang, C.; Yang, W.; Deng, J. Preparation and application of abietic acid-derived optically active helical polymers and their chiral hydrogels. *Bioresource Technol.* **2013**, *129*, 58–64.
15 Kouwer, P. H. J.; Koepf, M.; Le Sage, V. A. A.; Jaspers, M.; van Buul, A. M.; Eksteen-Akeroyd, Z. H.; Woltinge, T.; Schwartz, E.; Kitto, H. J.; Hoogenboom, R.; Picken, S. J.; Nolte, R. J. M.; Mendes, E.; Rowan, A. E. Responsive biomimetic networks from polyisocyanopeptide hydrogels. *Nature* **2013**, *493*, 651–655.
16 Das, R. K.; Gocheva, V.; Hammink, R.; Zouani, O.; Rowan, A. E. Stress-stiffening-mediated stem-cell commitment switch in soft responsive hydrogels. *Nat. Mater.* **2016**, *15*, 318–327.
17 Yuana, H.; Liu, K.; Cóndor, M.; Barrasa-Fano, J.; Louis, B.; Vandaele, J.; de Almeida, P.; Coucke, Q.; Chen, W.; Oosterwijk, E.; Xing, C.; Van Oosterwyck, H.; Kouwer, P. H. J.; Rocha, S. Synthetic fibrous hydrogels as a platform to decipher cell–matrix mechanical interactions. *Proc. Natl. Acad. Sci. U.S.A.* **2023**, *120*, e2216934120.
18 Yuan, H.; Liu, K.; van Velthoven, M. J. J.; Kumari, J.; Bao, Y.; Rocha, S.; Kouwer, P. H. J. Fibrous polyisocyanide hydrogels for 3D cell culture applications. *Nat. Protocols* **2025**, *20*, 3339–3360.
19 Wang, H.; Yong, X.; Huang, H.; Yu, H.; Wu, Y.; Deng, J. Chiral, thermal-responsive hydrogels containing helical hydrophilic polyacetylene: preparation and enantio-differentiating release ability. *Polym. Chem.* **2019**, *10*, 1780–1786.
20 Shen, L.; Cao, Y.; Wang, L.; Zhang, X.; Zhang, A.; Li, W. Compressible hydrogels with stabilized chirality from thermoresponsive helical dendronized poly(phenylacetylene)s. *Angew. Chem. Int. Ed.* **2024**, *63*, e202407552.
21 Wang, F.; Zhou, C.; Liu, K.; Yan, J.; Li, W.; Masuda, T.; Zhang, A. Thermoresponsive dendronized poly(phenylacetylene)s showing tunable helicity. *Macromolecules* **2019**, *52*, 8631–8642.
22 Lu, X.; Liu, Y.; Lu, D.; Xu, A.; Cao, Y.; Zhang, X.; Li, W.; Zhang, A. Thermoresponsive dendronized poly(phenylacetylene)s *via* dynamic covalent chemistry showing multiple-responsive chirality. *Macromolecules* **2023**, *56*, 10206–10221.
23 Ren, L.; Lu, X.; Li, W.; Yan, J.; Whittaker, A. K.; Zhang, A. Thermoresponsive helical dendronized poly(phenylacetylene)s: remarkable stabilization of their helicity *via* photo-dimerization of the dendritic pendants. *J. Am. Chem. Soc.* **2023**, *145*, 24906–24921.
24 Lu, X.; Ren, L.; Zhang, X.; Whittaker, A. K.; Li, W.; Zhang, A. Thermo/light dual-responsive helical dendronized poly(phenylacetylene)s. *Macromolecules* **2024**, *57*, 5915–5928.
25 Lu, X.; Wang, L.; Ren, L.; Li, W.; Zhang, A. thermoresponsive helical dendronized poly(arylacetylene)s: modulating the dynamic chirality. *Sci. China Chem.* **2025**, *68*, 1486–1496.
26 Sun, Z.; Zhang, Y.; Qiu, H.; Lu, X.; Ren, L.; Shen, L.; Zhang, A. Synthesis of helical poly(phenylacetylene)s carrying dendritic pendants with varied branching densities through polymerization in different solvents. *Chinese J. Polym. Sci.* **2023**, *41*, 1543–1554.
27 Wang, L; Jia, R.; Zhang, A.; Li, W. Sponge-like thermoresponsive hydrogels from helical dendronized poly(phenylacetylene)s as soft actuators. *Eur. Polym. J.* **2025**, *240*, 114357.
28 Li, W.; Zhang, A.; Feldman, K.; Walde, P.; Schlüter, A. D. Thermoresponsive dendronized polymers. *Macromolecules* **2008**, *41*, 3659–3667.
29 Junk, M. J. N.; Li, W.; Schluter, A. D.; Wegner, G.; Spiess, H. W.; Zhang, A.; Hinderberger, D. EPR spectroscopic characterization of local nanoscopic heterogeneities during the thermal collapse of

thermoresponsive dendronized polymers. *Angew. Chem., Int. Ed.* **2010**, *49*, 5683–5687.
30 Zhang, J.; Yan, Z.; Zhao, Q.; Su, X.; Whittaker, A. K.; Zhang, A.; Li, W. Enhanced confinements to modulate efficient reversible isomerization of donor-acceptor Stenhouse adducts in water through cooperative crowding in thermoresponsive dendronized nanogels. *Chem. Eng. J.* **2025**, *503*, 158518.
31 Gao, R.; Li, S.; Liu, N.; Liu, B.; Wu, Z. Helical polymers: from precise synthesis to structures and functions. *Chem. Rev.* **2026**, *126*, 297–403.
32 Gao, R.; Duan, B.; Zong, Y.; Liu, N.; Wu, Z. Controlled isocyanide polymerization: towards helical polymers with chiral functions. *Prog. Polym. Sci.* **2026**, *172*, 102056.
33 Zong, Y.; Gao, R.; Liu, N.; Lei, S.; Li, Z.; Wu, Z. Precise synthesis of telechelic rodlike polyisocyanides: versatile building blocks for fabricating polymer frameworks with controllable pore-apertures. *Chem. Sci.* **2026**, *17*, 255–264.
34 Gao, R.; Zong, Y.; Li, T.; Liu, N.; Wu, Z. Three-dimensional supramolecular polymer frameworks with precisely tunable and large apertures for enzyme encapsulation. *Chin. Chem. Lett.* **2026**, *37*, 111582.
35 Rowan, S. J.; Cantrill, S. J.; Cousins, G. R. L.; Sanders, J. K. M.; Stoddart, J. F. Dynamic covalent chemistry. *Angew. Chem. Int. Ed.* **2002**, *41*, 898–952.
36 Kim, J.; Hanna, J. A.; Hayward, R. C.; Santangelo, C. D. Thermally responsive rolling of thin gel strips with discrete variations in swelling. *Soft Matter* **2012**, *8*, 2375–2381.
37 Byun, M.; Santangelo, C. D.; Hayward, R. C. Swelling-driven rolling and anisotropic expansion of striped gel sheets. *Soft Matter* **2013**, *9*, 8264–8273.
38 Thérien-Aubin, H.; Wu, Z. L.; Nie, Z. H.; Kumacheva, E. Multiple shape transformations of composite hydrogel sheets. *J. Am. Chem. Soc.* **2013**, *135*, 4834–4839.
39 Yashima, E.; Maeda, K.; Okamoto, Y. Memory of macromolecular helicity assisted by interaction with achiral small molecules. *Nature* **1999**, *399*, 449–451.
40 Yashima, E.; Maeda, K. Chirality-responsive helical polymers. *Macromolecules* **2008**, *41*, 3–12.
41 Morino, K.; Maeda, K.; Yashima, E. Helix-sense inversion of poly(phenylacetylene) derivatives bearing an optically active substituent induced by external chiral and achiral Stimuli. *Macromolecules* **2003**, *36*, 1480–1486.
42 Wang, S.; Feng, X.; Zhang, J.; Yu, P.; Guo, Z.; Li, Z.; Wan, X. Helical conformations of poly(3,5-disubstituted phenylacetylene)s tuned by pendant structure and solvent. *Macromolecules* **2017**, *50*, 3489–3499.
43 He, C.; Yang, G.; Kuai, Y.; Shan, S.; Yang, L.; Hu, J.; Zhang, D.; Zhang, Q.; Zou, G. Dissymmetry enhancement in enantioselective synthesis of helical polydiacetylene by application of superchiral light. *Nat. Commun.* **2018**, *9*, 5117.
44 Lago-Silva, M.; Cid, M. M.; Quiñoá, E.; Freire, F. P/M macromolecular switch based on conformational control exerted by an achiral side chain within an axially chiral Locked pendant. *J. Am. Chem. Soc.* **2023**, *146*, 752–759.
45 Tarrío, J. J.; Rodríguez, R.; Crassous, J.; Quiñoá, E.; Freire, F. Conformational kinetics in chiral poly(diphenylacetylene)s: a dynamic *P/M* memory effect. *Angew. Chem. Int. Ed.* **2023**, *62*, e202307059.
46 Rey-Tarrío, F.; Rodríguez, R.; Quiñoá, E.; Freire, F. Screw sense excess and reversals of helical polymers in solution. *Nat. Commun.* **2023**, *14*, 1742.
47 Sun P. P.; Ren S. J.; Liu F. L.; Wu A. L.; Sun N.; Shi L. J.; Zheng L. Q. Smart low molecular weight hydrogels with dynamic covalent skeleton. *Soft Matter* **2018**, *14*, 6678–6683.
48 Hirokawa, Y.; Jinnai, H.; Nishikawa, Y.; Okamoto, T.; Hashimoto, T. Direct observation of internal structures in poly(N-isopropylacrylamide) chemical gels. *Macromolecules* **1999**, *32*, 7093–7099.
49 Kubota, R.; Tanaka, W.; Hamachi, I. Microscopic imaging techniques for molecular assemblies: electron, atomic force, and confocal microscopies. *Chem. Rev.* **2021**, *121*, 14281–14347.
50 Kenath, G. S.; Karanastasis, A. A.; Ullal, C. K.; Super-resolution imaging of spatial heterogeneities in model thermosensitive hydrogels with implications for their origins. *Macromolecules* **2021**, *54*, 7743–7753.
51 David, C.; de Souza, J. F.; Silva, A. F.; Grazioli, G.; Barboza, A. S.; Lund, R. G.; Fajardo, A. R.; Moraes, R. R. Cannabidiol-loaded microparticles embedded in a porous hydrogel matrix for biomedical applications. *J. Mater. Sci. Mater. Med.* **2024**, *35*, 14.